Proceeding of the IEEE
International Conference on Robotics and Biomimetics
Dali, China, December 2019

Dual Closed-loop Impedance Control for Wheeled Mobile Manipulator in Trajectory Tracking

Qirong Tang*, Pengjie Xu, Fangchao Yu, Jingtao Zhang and Zhipeng Xu
Laboratory of Robotics and Multibody System, School of Mechanical Engineering
Tongji University
Shanghai, China
qirong.tang@outlook.com

***Abstract*— This paper presents a dual closed-loop impedance control scheme for a nonholonomic wheeled mobile manipulator in trajectory tracking with nonlinear contact disturbance. The kinematics and dynamics models of the mobile platform and n-links manipulator are established based on the Euler-Lagrangian approach. In order to control and eliminate the influences caused by system uncertainties and nonlinear contact disturbance, a control scheme which consists of double closed loops is proposed. The impedance control is applied to realize force tracking control in the outer loop. The inner loop is then designed to deal with chattering of measured parameters by using extended Kalman filter. The proposed controller ensures the tracking error in workspace converges to zero and the input torques are smooth. Utilizing the Lyapunov method, the stability of the system is proved. Simulation compared with conventional control methods on two driving wheeled mobile manipulator shows the effectiveness and robustness of the proposed control scheme.**

***Index Terms*— Mobile manipulator, Dual closed-loop control, Kinematics and dynamics models, Extended Kalman filter.**

I. Introduction

Wheeled mobile manipulators (WMM) [1] has been studied by many researchers in the past decades. The WMM has a wide application prospect in construction, mining, and planetary sciences, due to its flexible function of manipulator's operation and mobile robot's extensity in workspace [2]. In practical application, two or even more mobile manipulators often complete a task in cooperation such as handling a heavy object, which makes it be a higher coupled nonlinear system [3]. In addition, the nonlinear contact force between the WMM and the object is crucial in the execution of tasks. Researchers found the WMM's kinematic and dynamic models are crucial for its control and task's execution [4].

Many researchers in this area focus on kinematic and dynamic modeling of mobile manipulators. Utilizing the forward recursive formulation, Yu and Chen proposed a general approach for kinemantic and dynamic modeling of nonholonomic mobile manipulator systems, which fully considers the existing equation and dynamic interactions of moving platform and manipulator [5]. However, there was no doubt that the dynamic model was complex by employing this method. In [6], the authors proposed an approach to transform complex dynamics of coordinated multiple WMMs into master and slave dynamics. The unknown input dead zones and delayed dynamics of the two subsystems were represented as linear time-varying and bounded disturbance system. However, the contact characteristics of the slave and object should be considered. To overcome the parameters coupling of nonholonomic wheeled mobile manipulator(NWMM), Brahmi et al. adopted a virtual decomposition control method to set up its dynamic model, which makes the control system more flexible when the configuration of NWMM changes [7]. But the uncertainties, high nonlinearity and coupling of system variables have been simplified or ignored. These researches performed effectively and improve gradually the work-efficiency of WMM. However, the nonlinear contact force was not solved, and the tight kinematics and dynamics coupling of systems is still existing.

In the past decades, a number of researchers had paid attention to the trajectory tracking control methods of WMMs, which can be mainly divided into decentralized and centralized. Seo and Han designed a dual closed-loop sliding mode control where the outer loop controlled the virtual velocity command and the inner loop can guarantee the convergence of position error not depending on tedious parameter identification [8]. Wang proposed an adaptive recurrent neural network control scheme to deal with the unknown dynamics and to eliminate the need for the error-prone proces [9], however the holonomic or nonholonomic dynamic model of mobile manipulators which based on this assumption was difficult to implement in practice. Considering the obstacle avoidance, a hybrid adaptive-fuzzy controler was presented in [10], however the real trajectory was dithering and halt, and the required speed was changed while avoiding obstacle. In the practical trajectory tracking of WMMs, not only the motion needs to be controlled but also the interaction with object should be considered. Moreover, in general, more information of system and external environment used in controller leads to better tracking performance.

Inspired by aforementioned literature, in this study we present an effective impedance control scheme of NWMM, which aims at dealing with the issue of realistic tracking with system uncertainties, coupled external nonlinear disturbances. The main work of this paper can be presented as follows:

978-1-7281-6321-5/19//$31.00 ©2019 IEEE

The kinematic and dynamic models first of all presented. The proposed dual closed-loop impedance control scheme can guarantee trajectory tracking effectively and rapidly, since extended Kalman filter (EKF) used in the inner loop to eliminate chattering and impedance control method is applied to deal with nonlinear contact disturbance in the outer control loop. The proposed controller has a simple structure and its stability can be proved based on the Lyapunov theory. Related application examples in simulation are presented.

The remaining of this paper is organized as follows. Section 2 addresses the kinematic and dynamic models of n-links NWMM, and Section 3 explains the dual closed-loop impedance control scheme with stability analysis detailedly. The simulation is given in Section 4. The conclusion is drawn in Section 5 finally.

II. SYSTEM MODELING

In this section, a n-links NWMM is depicted in Fig.1. The general kinematic and dynamic models are set up based on D-H method and the Euler-Lagrange method.

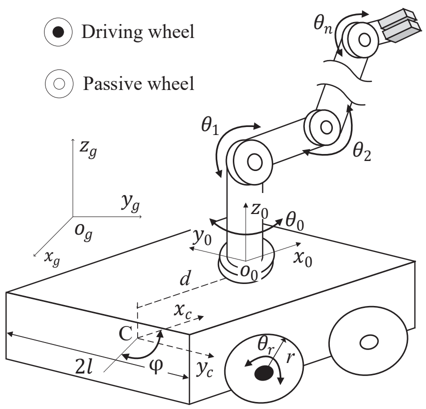

Fig. 1. The nonholonomic wheeled mobile manipulator system

As shown in Fig.1, point C is the central point of wheeled mobile platform, $\boldsymbol{P}_c = [x, y, \varphi]^T$ is the position and orientation of point C in the coordinate system $o_g - x_g\, y_g\, z_g$. Here $\theta_1 \cdots \theta_n$ are the angles of n-joints respectively. Let $\boldsymbol{q}_m = [\theta_1 \cdots \theta_n]^T$ be the joint variables in the coordinate system $o_g - x_g\, y_g\, z_g$. $c - x_c\, y_c$ is the platform reference frame, $o_{i-1} - x_{i-1}\, y_{i-1}\, z_{i-1}$ is the ith link's references frame. m_p is the mass of mobile platform, $m_1, \cdots, m_n$ are the mass of link 1 to link n, respectively.

A. Kinematic model

Let $\boldsymbol{P}_g = \left[\boldsymbol{P}_{\boldsymbol{c}}^T, \boldsymbol{P}_{\boldsymbol{m}}^T\right]^T = [x_c, y_c, \varphi, \theta_1, ..., \theta_n]^T$ be the position and orientation coordinate vector of n-links NWMM, and $\boldsymbol{q}_c = [\theta_r, \theta_l]^T$ be the angular displacement vector of mobile platform. Since nonholonomic constraints of mobile platform, the relation of $\boldsymbol{P}_c$ can be given as

$$\boldsymbol{A}\dot{\boldsymbol{P}}_c = 0, \tag{1}$$

where $\boldsymbol{A} = [-\sin(\varphi), \cos(\varphi), -d]$.

Then, the relationship between $\boldsymbol{P}_g$ and $\boldsymbol{q}_g = \left[\boldsymbol{q}_c^T, \boldsymbol{q}_m^T\right]^T = [\theta_r, \theta_l, \theta_1, ..., \theta_n]^T$ can be written as follows

$$\dot{\boldsymbol{P}}_g = \begin{bmatrix} \boldsymbol{S}_c & \boldsymbol{S}_{cm} \\ \boldsymbol{S}_{mc} & \boldsymbol{S}_m \end{bmatrix} \dot{\boldsymbol{q}}_g(\theta), \tag{2}$$

the matrix $\boldsymbol{S} \in R^{(n+3)\times(n+3)}$, $\boldsymbol{S}_c \in R^{3\times 3}$ is a basis in nullspace $\boldsymbol{A} \in R^{1\times(n+3)}$, that is $\boldsymbol{S}_c^T \boldsymbol{A}^T = 0$. $\boldsymbol{S}_{cm}, \boldsymbol{S}_{mc}$ and $\boldsymbol{S}_m$ are constant matrices.

The kinematics equations of n-links WMM is established by using D-H method, the coordinate transformation matrix ${}^g\boldsymbol{T}_0$ between the coordinate system $\{o_0\}$ and the global coordinate system $\{o_g\}$ can be expressed as

$${}^g\boldsymbol{T}_0 = {}^g\,\boldsymbol{T}_c\,{}^c\boldsymbol{H}_0, \tag{3}$$

where ${}^c\boldsymbol{H}_0$ is the translational transformation matrix between the coordinate system $\{o_c\}$ and the $\{o_0\}$ of n-links manipulator.

The pose matrix of end-effector in coordinate system $\{o_g\}$ is

$$\begin{bmatrix} \boldsymbol{n} & \boldsymbol{o} & \boldsymbol{a} & \boldsymbol{p} \end{bmatrix} = {}^g\,\boldsymbol{T}_0 \prod_{i=1}^{n} {}^{i-1}\boldsymbol{T}_i, \tag{4}$$

where matrix ${}^{i-1}\boldsymbol{T}_i$ describing positional and orientational relation of the $(i-1)$th link and ith link, position vector $\boldsymbol{n} = \begin{bmatrix} n_x & n_y & n_z & 0 \end{bmatrix}^T$.

The Jacobian matrix $\boldsymbol{J} \in R^{6\times(n+3)}$ describes position vector $\boldsymbol{P}_g = [x_c, y_c, \varphi, \theta_1, ..., \theta_n]^T$ and its derivation vector $\dot{\boldsymbol{P}}_g = \begin{bmatrix} \boldsymbol{v}^T & \boldsymbol{\omega}^T \end{bmatrix}^T \in 6 \times 1$ is got by using differential transformation method

$$\begin{bmatrix} \boldsymbol{v}^T & \boldsymbol{\omega}^T \end{bmatrix}^T = \boldsymbol{J}\dot{\boldsymbol{P}}_g, \tag{5}$$

where $\boldsymbol{v}^T = \begin{bmatrix} v_x & v_y & v_z \end{bmatrix}^T$ and $\boldsymbol{\omega} = \begin{bmatrix} \omega_x & \omega_y & \omega_z \end{bmatrix}^T$ are linear and angular velocity of end-effector respectively.

Substitute Eq. (2) into Eq. (5), we can obtain the relationship between $\boldsymbol{v}$, $\boldsymbol{\omega}$ and each joint velocity $\dot{\boldsymbol{q}}_g(\theta)$

$$\begin{bmatrix} \boldsymbol{v}^T & \boldsymbol{\omega}^T \end{bmatrix}^T = \boldsymbol{J} \begin{bmatrix} \boldsymbol{S}_c & \boldsymbol{S}_{cm} \\ \boldsymbol{S}_{mc} & \boldsymbol{S}_m \end{bmatrix} \dot{\boldsymbol{q}}_g(\theta) = \boldsymbol{J}\left[\boldsymbol{S}_D\right] \dot{\boldsymbol{q}}_g(\theta), \tag{6}$$

$\jmath = \boldsymbol{J}\left[\boldsymbol{S}_D\right]$ is used for citing conveniently.

The acceleration of the end-effector and the vector $\boldsymbol{q}_g$ is

$$\begin{bmatrix} \dot{\boldsymbol{v}}^T & \dot{\boldsymbol{\omega}}^T \end{bmatrix}^T = \dot{\jmath}\dot{\boldsymbol{q}} + \jmath\ddot{\boldsymbol{q}}. \tag{7}$$

B. Dynamic model

Dynamic model of n-links NWMM is established by using Euler-Lagrangian method, the kinematic energy can be expressed as

$$T = \frac{1}{2}m_c\left(\dot{x}^2 + \dot{y}^2\right) + \frac{1}{2}I_c\dot{\varphi}^2 + \frac{1}{2}m_i\sum_{i=1}^{n}\boldsymbol{v}_i^2 + \frac{1}{2}I_i\sum_{i=1}^{n}\boldsymbol{\omega}_i^2, \tag{8}$$

where I_c, I_i are the moment of inertia for mobile platform and n-links manipulator, respectively, where $\boldsymbol{v}_i$, $\boldsymbol{\omega}_i$ can be obtained by Eq. (5).

The potential energy of system is

$$V = m_c\, g\, \boldsymbol{p}_{cz} + g \sum_{i=1}^{n} m_i\, \boldsymbol{p}_{iz}, \tag{9}$$

where $\boldsymbol{p}_{cz}$ is determined by the structure of NWMM, $\boldsymbol{p}_{iz}$ can be calculated by Eq.(4).

By constructing Lagrange function $L = T - V$ and computing equation $\frac{\partial}{\partial t}\left(\frac{\partial L}{\partial \dot{P}}\right) - \frac{\partial L}{\partial P} = Q$, one gets the system dynamic equation subjected to nonholonomic constraint as

$$\boldsymbol{M}\left(\boldsymbol{P}\right)\ddot{\boldsymbol{P}}_g + \boldsymbol{C}\left(\boldsymbol{P}, \dot{\boldsymbol{P}}\right)\dot{\boldsymbol{P}}_g + \boldsymbol{G}\left(\boldsymbol{P}\right) + \boldsymbol{\tau}_d = \boldsymbol{B}\boldsymbol{\tau} - \boldsymbol{A}_0^T\boldsymbol{\lambda}, \tag{10}$$

where $\boldsymbol{M}\left(\boldsymbol{P}\right) \in R^{(n+3)\times(n+3)}$ is the inertia matrix, $\boldsymbol{C}\left(\boldsymbol{P}, \dot{\boldsymbol{P}}\right) \in R^{(n+3)\times(n+3)}$ is the matrix of centripetal and coriolis forces, $\boldsymbol{G}\left(\boldsymbol{P}\right) \in R^{(n+3)\times 1}$ represents the gravitational vector, $\boldsymbol{\tau_d} \in R^{(n+3)\times 1}$ is bounded unknow external disturbance and the modelling error, $\boldsymbol{B} \in R^{(n+3)\times(n+2)}$ is the input transformation matrix, $\boldsymbol{\tau} \in R^{(n+3)\times(n+3)}$ is the input fore or torque, $\boldsymbol{A_0^T} = \begin{bmatrix}\boldsymbol{A^T} & \boldsymbol{0}\end{bmatrix}^T \in R^{(n+3)\times 1}$ is nonholonomic constraint matrix defined in [8], $\boldsymbol{\lambda}$ is the Lagrange multiplier.

To gain dynamic equation about freedom state vector $\boldsymbol{q}_g = [\theta_r, \theta_l, \theta_1, ..., \theta_n]$, one takes the derivative of Eq. (2) and obtains

$$\ddot{\boldsymbol{P}}_g = \begin{bmatrix}\dot{\boldsymbol{S}}_c & \dot{\boldsymbol{S}}_{cm}\\ \dot{\boldsymbol{S}}_{mc} & \dot{\boldsymbol{S}}_m\end{bmatrix}\dot{\boldsymbol{q}}_g(\theta) + \begin{bmatrix}\boldsymbol{S}_c & \boldsymbol{S}_{cm}\\ \boldsymbol{S}_{mc} & \boldsymbol{S}_m\end{bmatrix}\ddot{\boldsymbol{q}}_g(\theta). \tag{11}$$

Substitute Eq. (2) and Eq. (11) into Eq. (10) and multiply both sides of Eq. (10) by $\boldsymbol{S}^T$, we can get the dynamic equations of NWMM

$$\tilde{\boldsymbol{M}}\left(\boldsymbol{q}\right)\ddot{\boldsymbol{q}} + \tilde{\boldsymbol{C}}\left(\boldsymbol{q}, \dot{\boldsymbol{q}}\right)\dot{\boldsymbol{q}} + \tilde{\boldsymbol{G}}\left(\boldsymbol{q}\right) + \tilde{\boldsymbol{\tau}}_d = \tilde{\boldsymbol{B}}\boldsymbol{\tau} - \tilde{\boldsymbol{A}}_0^T\boldsymbol{\lambda}, \tag{12}$$

where $\tilde{\boldsymbol{M}}\left(\boldsymbol{q}\right) = \boldsymbol{S}^T\boldsymbol{M}\left(\boldsymbol{P}\right)\boldsymbol{S} \in R^{(n+2)\times(n+2)}$, $\tilde{\boldsymbol{C}}\left(\boldsymbol{q}, \dot{\boldsymbol{q}}\right) = \boldsymbol{S}^T\boldsymbol{M}\left(\boldsymbol{P}\right)\dot{\boldsymbol{S}} + \boldsymbol{S}^T\boldsymbol{C}\left(\boldsymbol{q}, \dot{\boldsymbol{q}}\right)\boldsymbol{S} \in R^{(n+2)\times(n+2)}$, $\tilde{\boldsymbol{G}}\left(\boldsymbol{q}\right) = \boldsymbol{S}^T\boldsymbol{G}\left(\boldsymbol{P}\right) \in R^{(n+2)\times 1}$, $\tilde{\boldsymbol{\tau}}_d = \boldsymbol{S}^T\boldsymbol{\tau}_d \in R^{(n+2)\times(n+2)}$, $\tilde{\boldsymbol{B}} = \boldsymbol{S}^T\boldsymbol{B} \in R^{(n+2)\times 1}$, according to the analysis with similar concept in [11] the constraint forces term $\tilde{\boldsymbol{A}}_0^T\boldsymbol{\lambda}$ can be eliminated.

The following properties and assumptions are desired for Eq. (12).

***Property** 1:* The dynamic model is linear to these physical parameters of NWMM, that means if a vector $\boldsymbol{\zeta}$ is defined, we can get
$\tilde{\boldsymbol{M}}\left(\boldsymbol{q}\right)\ddot{\boldsymbol{q}} + \tilde{\boldsymbol{C}}\left(\boldsymbol{q}, \dot{\boldsymbol{q}}\right)\dot{\boldsymbol{q}} + \tilde{\boldsymbol{G}}\left(\boldsymbol{q}\right) = \boldsymbol{\Xi}\left(\boldsymbol{q}, \dot{\boldsymbol{q}}, \ddot{\boldsymbol{q}}\right)\zeta$, where $\boldsymbol{\Xi}\left(\boldsymbol{q}, \dot{\boldsymbol{q}}, \ddot{\boldsymbol{q}}\right)$ is positive definite matrix.

***Assumption** 1:* The full rank matrix $\boldsymbol{S}$, nonlinear external disturbance $\boldsymbol{\tau}_d$ and positive definite matrix $\boldsymbol{\Xi}$ are bounded, respectively, that is,
$\|\boldsymbol{S}\| \leq \boldsymbol{S}_\varepsilon$, $\|\boldsymbol{\tau}_d\| \leqslant \boldsymbol{\tau}_\varepsilon$, $\|\boldsymbol{\Xi}_q\| \leqslant \boldsymbol{\Xi}_\varepsilon$,
where $\boldsymbol{S}_\varepsilon$, $\boldsymbol{\tau}_\varepsilon$ and $\boldsymbol{\Xi}_\varepsilon$ are positive constants.

III. Dual Closed-loop Impedance Control

The proposed dual closed-loop impedance control scheme is introduced completely in this section. It contains two aspects. First, the controller is proposed. Then, the stability and convergence of the proposed controller are analyzed based on the Lyapunov theory.

A. Controller design

The structure of the proposed controller is shown in Fig.2, which is in terms of the composition of two closed control loops. Inner loop controller is designed for NWMM to follow reference trajectory efficiently by applying EKF. Expected equivalent impedance parameters $\boldsymbol{x}_i$, $\dot{\boldsymbol{x}}_i$ and $\ddot{\boldsymbol{x}}_i$ are generated by outer loop controller, which aimed to get new impedance tracking trajectory. In this way, the track can be much smoother than the original track, furthermore the precision of the position is higher.

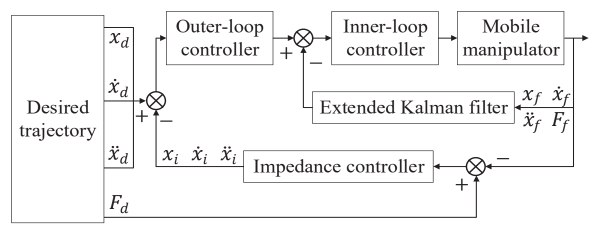

Fig. 2. The dual closed-loop impedance control system

The impedance force error $\boldsymbol{e}_f$ between the feedback force $\boldsymbol{F}_f$ and desired force $\boldsymbol{F}_d$ is calculated as

$$\boldsymbol{M}_i\left(\Delta\ddot{\boldsymbol{x}}_i\right) + \boldsymbol{C}_i\left(\Delta\dot{\boldsymbol{x}}_i\right) + \boldsymbol{K}_i\left(\Delta\boldsymbol{x}_i\right) = \boldsymbol{F}_d - \boldsymbol{F}_f, \tag{13}$$

where $\boldsymbol{M}_i$, $\boldsymbol{C}_i$ and $\boldsymbol{K}_i$ are the inertia, damping and stiffness target impedance parameter matrix, respectively, $\ddot{\boldsymbol{x}}_i$, $\dot{\boldsymbol{x}}_i$, $\boldsymbol{x}_i$ are equivalent impedance correction position, velocity and acceleration, respectively, $\boldsymbol{F}_d$ is the desirable force. $\boldsymbol{F}_f$ is feedback force.

***Property** 2:* The dynamic model is linear to physical parameters of NWMM, that is defined a vector $\boldsymbol{\zeta_i}$, we can get
$\boldsymbol{M}_i\left(\Delta\ddot{\boldsymbol{x}}_i\right) + \boldsymbol{C}_i\left(\Delta\dot{\boldsymbol{x}}_i\right) + \boldsymbol{K}_i\left(\Delta\boldsymbol{x}_i\right) = \Xi_i\boldsymbol{\zeta_i}$, where Ξ_i is positive definite matrix.

***Assumption** 2:* The positive definite matrix Ξ_i is bounded, that is, $\|\Xi_i\| \leqslant \Xi_{i\varepsilon}$, where $\Xi_{i\varepsilon}$ is positive constant.

To eliminate chattering in the trajectory tracking, we designed an inner loop controller based on EKF.

$$\begin{cases} \hat{x}_k = \tilde{x}_k + K_k\left(x_k - \tilde{x}_k\right)\\ \hat{\dot{x}}_k = \tilde{\dot{x}}_k + K_k\left(\dot{x}_k - \tilde{\dot{x}}_k\right)\\ \hat{\ddot{x}}_k = \tilde{\ddot{x}}_k + K_k\left(\ddot{x}_k - \tilde{\ddot{x}}_k\right)\\ \hat{F}_k = \tilde{F}_k + K_k\left(F_k - \tilde{F}_k\right) \end{cases} \tag{14}$$

where x_k, $\dot{x}_k$, $\ddot{x}_k$ and F_k are the observation variables, $\tilde{x}$, $\tilde{\dot{x}}_k$, $\tilde{\ddot{x}}_k$ and $\tilde{F}_k$ are the posteriori estimations respectively.

Define the tracking errors $\boldsymbol{e} = \boldsymbol{x}_o - \boldsymbol{x}$, $\dot{\boldsymbol{e}} = \dot{\boldsymbol{x}}_o - \dot{\boldsymbol{x}}$ and the sliding surface $\boldsymbol{s}$ can be denoted as

$$\boldsymbol{s} = \boldsymbol{\Lambda}_1 \dot{\boldsymbol{e}} + \boldsymbol{\Lambda}_2 \boldsymbol{e}, \tag{15}$$

where $\boldsymbol{\Lambda}_1$, $\boldsymbol{\Lambda}_2$ are positive gain matrices.

Differentiate Eq.(15) in time and multiply $\tilde{\boldsymbol{M}}$ in the both sides

$$\begin{aligned}
\tilde{\boldsymbol{M}}\dot{\boldsymbol{s}} &= \tilde{\boldsymbol{M}}\boldsymbol{\Lambda}_1\ddot{\boldsymbol{x}}_0 - \tilde{\boldsymbol{M}}\boldsymbol{\Lambda}_1\ddot{\boldsymbol{x}} + \tilde{\boldsymbol{M}}\boldsymbol{\Lambda}_2\dot{e} \\
&= \tilde{\boldsymbol{M}}\boldsymbol{\Lambda}_1\ddot{\boldsymbol{x}}_d - \tilde{\boldsymbol{M}}\boldsymbol{\Lambda}_1\Delta\ddot{\boldsymbol{x}}_i - \boldsymbol{B}\boldsymbol{\tau} + \boldsymbol{C}(\boldsymbol{q},\dot{\boldsymbol{q}})\dot{\boldsymbol{P}}_g \\
&\quad + \boldsymbol{G}(\boldsymbol{q}) + \boldsymbol{\tau}_d + \tilde{\boldsymbol{M}}\boldsymbol{\Lambda}_2(\ddot{\boldsymbol{x}}_d - \Delta\ddot{\boldsymbol{x}}_i - \ddot{\boldsymbol{x}}) \\
&= \tilde{\boldsymbol{M}}(\boldsymbol{q})(\boldsymbol{\Lambda}_1 + \boldsymbol{\Lambda}_2)\ddot{\boldsymbol{x}}_d + \boldsymbol{C}(\boldsymbol{q},\dot{\boldsymbol{q}})(\dot{\boldsymbol{x}}_d + \boldsymbol{\Lambda}_2\boldsymbol{e}) \\
&\quad + \boldsymbol{G}(\boldsymbol{q}) - \tilde{\boldsymbol{M}}_i\boldsymbol{\Lambda}_1\Delta\ddot{\boldsymbol{x}}_i - \bar{\boldsymbol{C}}_i\dot{\boldsymbol{x}}_i - \boldsymbol{B}\tau \\
&\quad - \boldsymbol{\Lambda}_2^{-1}\boldsymbol{C}\left(\boldsymbol{P},\dot{\boldsymbol{P}}\right)\boldsymbol{s} + \boldsymbol{\tau}_d
\end{aligned}. \tag{16}$$

According to Eq.(16), the controller τ can be defined as

$$\tau = \boldsymbol{B}^{-1}(\boldsymbol{\tau}_q + \boldsymbol{\tau}_i + \boldsymbol{\tau}_s), \tag{17}$$

where

$$\begin{cases}
\boldsymbol{\tau}_q = \tilde{\boldsymbol{M}}(\boldsymbol{q})(\boldsymbol{\Lambda}_1 + \boldsymbol{\Lambda}_2)\ddot{\boldsymbol{x}}_d \\
\qquad + \boldsymbol{C}(\boldsymbol{q},\dot{\boldsymbol{q}})(\dot{\boldsymbol{x}}_d + \boldsymbol{\Lambda}_2\boldsymbol{e}) + \boldsymbol{G}(\boldsymbol{q}) \\
\boldsymbol{\tau}_i = -\tilde{\boldsymbol{M}}_i\boldsymbol{\Lambda}_1\Delta\ddot{\boldsymbol{x}}_i - \bar{\boldsymbol{C}}_i\dot{\boldsymbol{x}}_i \\
\boldsymbol{\tau}_s = \boldsymbol{\Re}\boldsymbol{sgn}(\boldsymbol{s}) = \boldsymbol{S}_\varepsilon\boldsymbol{\tau}_\varepsilon\boldsymbol{sgn}(\boldsymbol{s})
\end{cases},$$

$\boldsymbol{\Re}$ is a positive gain.

Up to now, the trajectory tracking problem in presence of parametric uncertainties and external nonlinear disturbance can be solved by using proposed control torque input $\boldsymbol{\tau}$ in Eq.(14). the position vector in inner loop can smoothly follow the desired impedance trajectories due to EKF and sliding mode control approach. The problem of tracking precision, which generating by actual nonlinear contact force in the process of trajectory tracking, can be also effectively guaranteed by impedance control torque input $\boldsymbol{\tau_i}$.

B. Stability analysis

The stability analysis of proposed controller is performed. First a Lyapunov function is chosen

$$\boldsymbol{V} = \frac{1}{2}\boldsymbol{s}^T\tilde{\boldsymbol{M}}(\boldsymbol{q})\boldsymbol{s}. \tag{18}$$

Next, we differentiate Eq. (18) in time, and then substitute Eq. (17) and relevant **Properties** (1 and 2) and **Assumptions** (1 and 2),

$$\begin{aligned}
\dot{\boldsymbol{V}} &= \boldsymbol{s}^T\tilde{\boldsymbol{M}}(\boldsymbol{q})\dot{\boldsymbol{s}} + \frac{1}{2}\boldsymbol{s}^T\dot{\tilde{\boldsymbol{M}}}\boldsymbol{s} \\
&= \boldsymbol{s}^T[\tilde{\boldsymbol{M}}(\boldsymbol{q})(\boldsymbol{\Lambda}_1 + \boldsymbol{\Lambda}_2)\ddot{\boldsymbol{x}}_d + \boldsymbol{C}(\boldsymbol{q},\dot{\boldsymbol{q}})(\dot{\boldsymbol{x}}_d + \boldsymbol{\Lambda}_2\boldsymbol{e}) \\
&\quad + \boldsymbol{G}(\boldsymbol{q}) - \tilde{\boldsymbol{M}}_i\boldsymbol{\Lambda}_1\Delta\ddot{\boldsymbol{x}}_i - \bar{\boldsymbol{C}}_i\dot{\boldsymbol{x}}_i - \boldsymbol{B}\tau + \boldsymbol{\tau}_d \\
&\quad - \boldsymbol{\Lambda}_2^{-1}\boldsymbol{C}\left(\boldsymbol{P},\dot{\boldsymbol{P}}\right)\boldsymbol{s} + \frac{1}{2}\boldsymbol{s}^T\left\{\dot{\tilde{\boldsymbol{M}}}(\boldsymbol{q}) - 2\tilde{\boldsymbol{C}}(\boldsymbol{q},\dot{\boldsymbol{q}})\right\}\boldsymbol{s} \\
&\leqslant \boldsymbol{s}^T[\boldsymbol{\Xi}_q + \boldsymbol{\Xi}_i + \boldsymbol{\Re}] \\
&= \sum_{i=1}^{n}\left\{\boldsymbol{s}_i(\boldsymbol{\Xi}_q) - \boldsymbol{s}_i(\boldsymbol{\Xi}_i) - \boldsymbol{s}^T\boldsymbol{\Re}\boldsymbol{sgn}(\boldsymbol{s})\right\} \\
&= -\sum_{i=1}^{n}(\boldsymbol{\Re}_i\|\boldsymbol{s}_i\|) \leqslant 0\ .
\end{aligned} \tag{19}$$

In Eq. (19), $\boldsymbol{\Re} = \boldsymbol{diag}[\Re_1, \Re_2, \cdots, \Re_{n+2}]$, $\boldsymbol{sgn}(s) = [sgn(s_1), sgn(s_2), \cdots, sgn(s_{n+2})]$. In Eq. (18) and Eq. (19), $\boldsymbol{V} \geqslant 0$ and $\dot{\boldsymbol{V}} \leqslant 0$, respectively, therefore the tracking errors are converged and the stability of the dual closed-loop impedance control scheme with system coupling and disturbance can be guaranteed.

IV. SIMULATION

In this section, in order to verify the effectiveness of the proposed controller, simulation on a mobile platform with two DOF manipulators are carried out, whose dynamic parameters are same as those in Ref. [12] and dynamic parameters are listed in TABLE I.

TABLE I
PARAMETERS OF THE WMM SYSTEMS

Symbol	Parameter	Value
m_p, m_r, m_1	mass of body, wheels	$5kg$, $0.58kg$
m_1	mass of link1, link2	$0.5kg$, $0.45kg$
l_1	length of link1	$110mm$
d	horizontal distance of point C and point o_0	$145mm$
$2l$	distance of the wheels	$400mm$
r	radius of wheels	$75mm$

According to Eq. (4), we can obtain the moving trail, velocity and acceleration of the end-effector. Figure 3 expresses a moving trail of NWMM which is an involute helicoidal line rotating along the z axis. The motion relations of each degree of freedom in the Cartesian space can also be solved by the inverse kinematics.

External nonlinear contact disturbance $\boldsymbol{\tau}_d$ without loss of universality and applicability is described as

$$\boldsymbol{\tau}_d = \begin{cases} \begin{bmatrix}\boldsymbol{M}_m\ddot{\boldsymbol{x}} & \boldsymbol{B}_m\dot{\boldsymbol{x}} & \boldsymbol{K}_m\boldsymbol{x}\end{bmatrix}^T & if\ x \geqslant 2 \\ \begin{bmatrix}\boldsymbol{\tau}_x & \boldsymbol{\tau}_y & \boldsymbol{\tau}_z\end{bmatrix}^T & if\ x < 2 \end{cases}, \tag{20}$$

where $\boldsymbol{M}_m$, $\boldsymbol{B}_m$ and $\boldsymbol{K}_m$ are damping parameters matrices of external obstacles. Here $\begin{bmatrix}\boldsymbol{\tau}_x & \boldsymbol{\tau}_y & \boldsymbol{\tau}_z\end{bmatrix}^T = \begin{bmatrix}5sin(0.2\pi t) & 4cos(0.8\pi t) & 3cos(0.2\pi t)\end{bmatrix}^T$ is white Gaussian noises.

In addition, PID controller and closed-loop sliding mode controller are compared to proposed controller. The relevant parameters of PID control law in the simulation are set as $k_p = 100$, $k_i = 20$ and $k_d = 15$. The parameter of SMC in Eq.

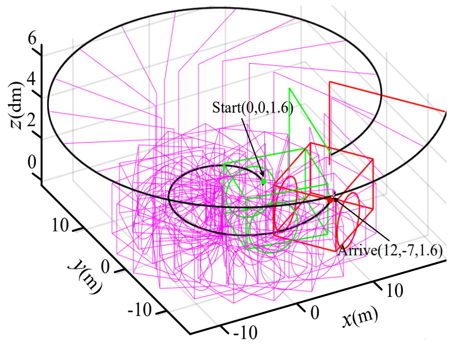

Fig. 3. The generated trajectory for NWMM

(17) is chosen as $\Re = \boldsymbol{diag}\{150, 150, 50, 50\}$. In the simulation, select the dual closed-loop impedance control parameters as, $\Re = \boldsymbol{diag}\{150, 150, 50, 50\}$. $\boldsymbol{q}_0 = \begin{bmatrix} 0 & 0 & 16 & 0 \end{bmatrix}^T$ and $\dot{\boldsymbol{q}}_0 = \begin{bmatrix} 0 & 0 & 0 & 0 \end{bmatrix}^T$ are the initial position and velocity, respectively. In this paper, other parameters are the same [8].

The simulation result shows in Figs.4-7. The tracking results of PID, SMC and proposed controllers along desired trajectory on coordinate system $o - xyz$ is shown in Fig. 3. Tracking trajectories in each direction are shown in Fig .4. Tracking errors of mobile platform and link 1 are shown in Fig. 5, respectively. The desired control torques of the three controllers are presented in Fig. 6.

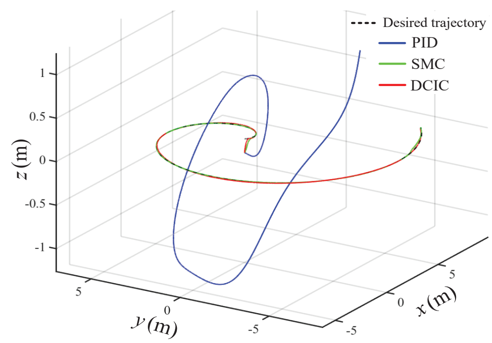

Fig. 4. The tracking trajectories in 3D presentation

Statistics are used to quantify the control performance, the maximum, mean and variance of tracking errors $\boldsymbol{e}$ in each direction can be calculated by Eq. (21). $L^2(\tau)$ is applied to solve chatting of the control input $\boldsymbol{\tau}_d$ shown in Eq. (22),

$$\begin{cases} e_{max} = [e_i]_{max} \\ \bar{e} = \sum_{t=0}^{T} e_i / T \\ s_e^2 = \sum_{t=o}^{T} e_i^T e_i / T \end{cases}, \tag{21}$$

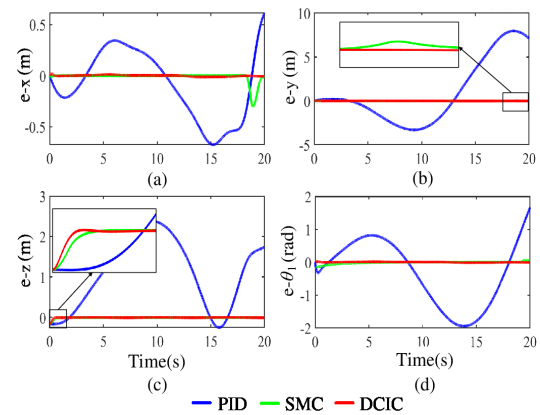

Fig. 5. The tracking errors in each direction

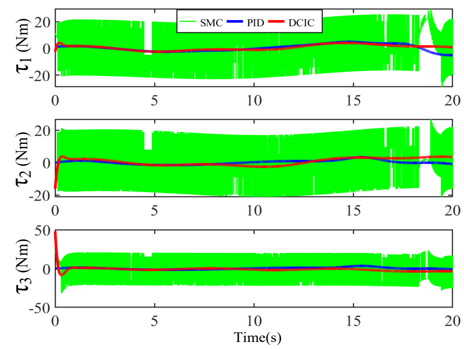

Fig. 6. The control torques of different control scheme

where T is the total simulation time.

$$L^2(\boldsymbol{\tau}) = \sum_{t=o}^{T} [\boldsymbol{\tau}_i - \bar{\boldsymbol{\tau}}]^T [\boldsymbol{\tau}_i - \bar{\boldsymbol{\tau}}] / T, \tag{22}$$

where $\bar{\boldsymbol{\tau}}$ is the mean of the control input.

From those figures and TABLE II, the tracking and their tracking errors can explain that the system which used the proposed controller converges to the desired trajectories quickly and achieves a better tracking performance. The proposed controller has a much faster convergence than PID and SMC by comparing the initial positions in Fig. 4 and Fig. 5(c). In addition, there is a bigger abruptly tracking error at about eighteenth second that is because the nonlinear contact

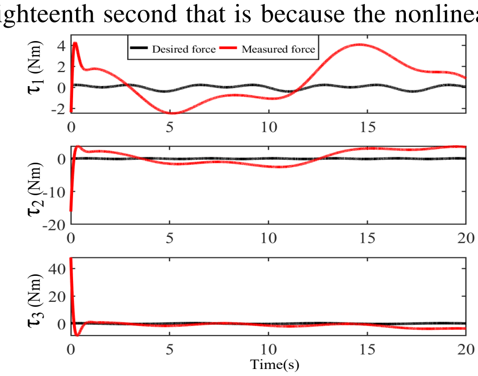

Fig. 7. The desired and measured torques of DCIC

TABLE II

STATISTICS OF TRACKING ERROR

System	Indices	Value
PID	e_{max} of x,y,z	0.6118, 7.9654, 2.3811
	$\bar{e}_x$, $\bar{e}_y$, $\bar{e}_z$,	-0.0902, 0.9431, 1.1056
	s_{ex}^2, s_{ey}^2, s_{ez}^2,	14.4627, 0.1212, 1.9920
	L_x^2, L_y^2, L_z^2,	6.9568, 1.5738, 1.5738
SMC	e_{max} of x,y,z	0.0817, 0.0390, 0.0023
	$\bar{e}_x$, $\bar{e}_y$, $\bar{e}_z$,	-0.0114, 0.0890, -0.0293
	s_{ex}^2, s_{ey}^2, s_{ez}^2,	0.0024, 0.0018, 0.0030
	L_x^2, L_y^2, L_z^2,	185.09, 171.45, 320.87
DCIC	e_{max} of x,y,z	0.0025, 0.002, 0.0054
	$\bar{e}_x$, $\bar{e}_y$, $\bar{e}_z$,	0.0020, -0.0011, -0.0019
	s_{ex}^2, s_{ey}^2, s_{ez}^2,	0.0014, 0.0005, 0.0021
	L_x^2, L_y^2, L_z^2,	0.0395, 0.0051, 0.0045

disturbance $\boldsymbol{\tau}_d$ changes. As shown in Fig. 5 and TABLE II , the tracking error of proposed control is the smallest which can show the proposed controller with a better robustness and stability.

It can be easily seen that the torque of PID and the dual closed-loop impedance control scheme is more smoothly, however the PID control law can't achieve trajectory tracking with the desired accuracy. The torque control input of SMC has a serious chattering phenomenon which will impact the actual control result.

There are a little errors or fluctuations relative to desired force, particularly after 15 seconds in the simulating process. That may be the impedance control torque input $\boldsymbol{\tau}_i$ acted on outer control loop to eliminate tracking errors causing by external nonlinear contact disturbance $\boldsymbol{\tau}_i$. In general, the proposed scheme has a reasonable breadth and practicability in the presence of nonlinear external disturbance.

V. CONCLUSIONS

This paper presents a dual closed-loop impedance control scheme for NWMM under external nonlinear contact disturbance. The kinematic and dynamic modelling of mobile platform and n-links manipulators has been given in detail. Then, aiming at eliminating the adverse impact of nonlinear external contact and uncertain disturbance, an effective control scheme consisting of EKF and impedance control method is proposed based on sliding mode control method. Additionally, the stability of the system is proved by the Lyapunov method. The proposed controller ensures that the tracking obtains faster convergence and the input force is bounded and stable. Comparative simulation with other control methods shows the effectiveness and better performance of the proposed method.

ACKNOWLEDGMENT

This work is supported by the projects of National Natural Science Foundation of China (No. 61603277, No. 61873192, No. 61733001), the Key Pre-Research Project of the 13th-Five-Year-Plan on Common Technology (No. 41412050101) and Field Fund (No. 61403120407). Meanwhile, this work is also partially supported by the Fundamental Research Funds for the Central Universities, and the Youth 1000 program project. It is also partially sponsored by the projects of Shanghai Science and Technology Innovation Plan (No. 15PJ1408400 No. 15JC1403300, No. 19510711100), as well as the projects supported by China Academy of Space Technology and Launch Vehicle Technology. All these supports are highly appreciated.

REFERENCES

[1] Tsingiuan Tsayjames and Peijiun Huang. Behavioristic image-based pose control of mobile manipulators using an uncalibrated eye-in-hand vision system. *Artificial Life & Robotics*, 23(1):94–102, 2018.

[2] MaiThang Long and Yaonan Wang. Adaptive position tracking system and force control strategy for mobile robot manipulators using fuzzy wavelet neural networks. *Journal of Intelligent & Robotic Systems*, 79(2):175–195, 2015.

[3] Mirosaw Galicki. Real-time constrained trajectory generation of mobile manipulators. *Robotics & Autonomous Systems*, 78:49–62, 2016.

[4] Giovanni Buizza Avanzini and Paolo Rocco. Constraint-based model predictive control for holonomic mobile manipulators. In *IEEE/RSJ International Conference on Intelligent Robots & Systems*, pages 1473–1479, Hamburg, Germany, September 28–30 2015.

[5] Qing Yu. A general approach to the dynamics of nonholonomic mobile manipulator systems. *Journal of Dynamic Systems Measurement and Control-transactions of The Asme*, 124(4):512–521, 2002.

[6] Zhijun Li and Zhuping Wang. Robust adaptive control of coordinated multiple mobile manipulators. *Mechatronics*, 18(5):239–250, 2008.

[7] Abdelkrim Brahmi, Maarouf Saad, Guy Gauthier, Wenhong Zhu, and Jawhar Ghommam. Adaptive control of multiple mobile manipulators transporting a rigid object. *International Journal of Control Automation and Systems*, 15(4):1779–1789, 2017.

[8] In Seok Seo and Seong Ik Han. Dual closed-loop sliding mode control for a decoupled three-link wheeled mobile manipulator. *Isa Transactions*, 80:322–335, 2018.

[9] Zhuping Wang and Tao Zhou. Adaptive recurrent neural network control of uncertain constrained nonholonomic mobile manipulators. *International Journal of Systems Science*, 45(2):133–144, 2014.

[10] Amal Karray, Malek Njah, Moez Feki, and Mohamed Jallouli. Intelligent mobile manipulator navigation using hybrid adaptive-fuzzy controller. *Computers & Electrical Engineering*, 56:773–783, 2016.

[11] Kerui Xia, Haibo Gao, Ding Liang, Guangjun Liu, Zongquan Deng, Liu Zhen, and Changyou Ma. Trajectory tracking control of wheeled mobile manipulator based on fuzzy neural network. *Neural Computing & Applications*, pages 1–16, 2016.

[12] Zhijun Li, Yipeng Yang, and Jianxun Li. Adaptive motion/force control of mobile under-actuated manipulators with dynamics uncertainties by dynamic coupling and output feedback. *IEEE Transactions on Control Systems Technology*, 18(5):1065–1079, 2010.